A lower crust origin for some flood basalts of the Emeishan large igneous province, SW China

J. GREGORY SHELLNUTT[1]*, TADASHI USUKI[2], ALLEN K. KENNEDY[3] & HAN-YI CHIU[1]

[1]National Taiwan Normal University, Department of Earth Sciences, 88 Tingzhou Road Academia Road Section 4, Taipei 11677, Taiwan

[2]Academia Sinica, Institute of Earth Sciences, 128 Academia Road Section 2, Taipei 11529, Taiwan

[3]Curtin University, Department of Applied Physics, Kent Street, Bentley, Western Australia 6102, Australia

**Corresponding author (e-mail: jgshelln@ntnu.edu.tw)*

Abstract: High seismic velocity layers within the lower crust (i.e. ~40 km) of the Yangtze Block are interpreted as mafic underplated rocks derived from the Emeishan mantle plume. However the region experienced a previous magmatic event during the Neoproterozoic (~800 Ma) which produced the Kangdian basalts and associated mafic intrusions. The identification of inherited Neoproterozoic (i.e. ~750 to ~850 Ma) zircons within Emeishan magmatic rocks indicates they either assimilated older material during emplacement or that they were derived from Neoproterozoic basement rocks of the Yangtze Block. Equilibrium partial melt modeling of Neoproterozoic Kangdian basalts can produce compositions similar to Emeishan basalt at a pressure of 1.2 GPa (i.e. ~40 km depth). The models indicate that is possible some magmatic rocks, including the flood basalts, of the ELIP are the product of partial melting of Neoproterozoic mafic rocks that underplated the lower crust of the Yangtze Block. Thus it is possible that some Emeishan basalts are the product of mafic lower crust recycling.

Supplementary material: The results of MELTS modeling are available at www.geolsoc.org.uk/SUPXXX

The Late Permian Emeishan flood basalts of SW China are the most voluminous rock-type of the Emeishan large igneous province (ELIP) which is one of at least five major eruptions of mafic continental volcanic rocks that occurred during the Late Palaeozoic (i.e. Tarim LIP, Siberian Traps, Panjal Traps, Skagerrak-Centred LIP). Like many continental flood basalts they are compositionally divided into 'high-Ti' and 'low-Ti' groups which are interpreted to reflect different petrological origins. The 'high-Ti' (i.e. TiO_2 > 2.5 wt%) basalts are interpreted to be derived by low degrees (< 8%) of partial melting of a mantle plume source whereas the formation of the 'low-Ti' basalts (i.e. TiO_2 < 2.5 wt%) is more complex and are suggested to be derived from the sub-continental lithospheric mantle (SCLM), or picritic magmas that assimilated upper crust, or the same source as the high-Ti basalts but merely represent higher degrees (i.e. 10-15%) of partial melting (Xu *et al*. 2001; Song *et al*. 2001, 2004, 2008a, b; Hanski *et al*. 2004; Xiao *et al*. 2004; Hou *et al*. 2006; Wang *et al*. 2007; Fan *et al*. 2008; Zhou *et al*. 2008; Shellnutt & Jahn 2011; Wang *et al*. 2011).

The ELIP is considered to be one of the best examples of a mantle plume derived large igneous province because there is evidence for pre-volcanic uplift, presence of ultramafic volcanic rocks (i.e. picrites), and short eruption duration of voluminous flood basalts (He *et al*. 2003; Hanski *et al*. 2004; Ali *et al*. 2005; Campbell 2005, 2007; Shellnutt *et al*. 2012; Shellnutt 2014). One of the most intriguing interpretations of the ELIP mantle plume model is related to the identification of high seismic velocity layers within the lower crust of the Yangtze Block beneath the region considered to be the epicenter of magmatism. The same region is interpreted to have thicker average crust than other regions of the western Yangtze Block (Xu *et al*. 2004; Xu and He 2007; Chen *et al*. 2010). Xu *et al*. (2004) interpreted the deep (i.e. > 100 km) high seismic velocity layers to be the fossilized Emeishan mantle plume head whereas the lower crust (i.e. 40 km to 60 km) high velocity layers are interpreted to be the underplated mafic and ultramafic rocks which fed the surface flows and shallow crustal intrusions. The seismic data interpretations coupled with the crustal thickness is a compelling explanation for and is consistent with the expectation of a mantle plume-derived large igneous province. However there is another equally valid interpretation of the high seismic velocity layers if they represent underplated mafic rocks.

The western margin of the Yangtze Block was the site of either long-lived subduction-related magmatism or mantle plume-related magmatism during the Neoproterozoic (Li *et al*. 1999; Zhou *et al*. 2002a, b; Zhao & Zhou 2007). The Neoproterozoic (~800 Ma) Kangdian basalts are located at the western boundary of the Yangtze Block within the Kangdian rift and are found within the same geographic area as the Emeishan basalts. The basalts and associated mafic dykes and plutonic rocks are described by Li *et al*. (2002) as being compositionally similar to continental flood basalts from Ethiopia and/or alkali basalts of Hawaii. In the case of the Kangdian basalts, they are interpreted to be derived from an OIB-like mantle plume source associated with the break-up of Rodina whereas similarly aged granitic rocks and younger (i.e. ~750 Ma) gabbros in the same region are interpreted to be related to an active continental margin setting (Li *et al*. 2002, 2005, 2006; Zhou *et al*. 2002a, b; Zhou *et al*. 2004; Lin *et al*. 2007; Zhao & Zhou 2007; Zhao *et al*. 2008; Wang *et al*. 2009; Wang *et al*. 2010). Regardless of how the Kangdian or other Neoproterozoic rocks formed (i.e. subduction zone setting vs. mantle plume), it is possible that magmas accumulated in the lower crust of the Yangtze Block and thus the crustal seismic layers may not be completely attributed to the ELIP. In fact, the seismic layers could represent a mixture of mafic and ultramafic material from both the Kangdian event and the Emeishan event.

In this paper we show the results of *in situ* zircon U/Pb dating and Hf isotopes of inherited Neoproterozoic zircons from Late Permian granitic rocks of the ELIP. We discuss the origins of the older zircons and evaluate the possibility that some ELIP-related magmatic rocks, including the flood basalts, may be derived by partial melting of rocks similar in composition to the Neoproterozoic Kangdian basalts.

Geological Background

The Late Permian Emeishan large igneous province (ELIP) is located in southwestern China on the western edge of the Yangtze Block near the boundary with the Early Triassic Songpan-Ganze terrane (Fig. 1a). The distribution of ELIP rocks was affected by faulting associated with the accretion of the Songpan-Ganze terrane and later during the Paleogene collision of India and Eurasian and covers an area of at least 0.3×10^6 km^2 including the Song Da zone of northern Vietnam which was translated ~600 km along the Ailao Shan-Red River shear zone during the Oligocene (Chung & Jahn 1995; Chung *et al*. 1997). The ELIP is subdivided into three structural zones (i.e. inner, intermediate and outer) based on crustal thickness estimates using seismic profiling (Figs. 1a, b). The inner zone of the ELIP is interpreted to have the thickest crust which thins radial to the outer zone (Xu *et al*. 2004). The volcanic succession ranges from a maximum thickness of ~5 km in the inner zone to < 1km at the margin of the outer zone. The volcanic rocks consist mostly of flood basalts but there is a higher proportion of picrites found in the lower flows of the inner zone whereas basaltic andesites and silicic volcanic rocks are common within the upper flows throughout the ELIP. The inner zone, chiefly the Panxi region, contains many giant orthomagmatic Fe-Ti-V oxide deposits whereas Ni-Cu-(PGE) and PGE deposits are found within the inner zone and outer zone but none have been found within the intermediate yet (Shellnutt 2014). The Yangtze Block was located at equatorial latitudes of eastern Pangaea and the volcanic rocks of the ELIP erupted on top of middle Permian limestones or directly on to Precambrian cratonic rocks.

The granitic plutons of this study are from the Song Da zone of northern Vietnam and the Panxi region in Sichuan. Northern Vietnam is part of the South China block, which is separated from the Indochina block by the Song Ma suture zone to the southwest (Fig. 1). The SW side of the ASRR shear zone consists of the Phan Si Pan uplift and Tu Le basin, which are further surrounded by Song Da belt in the west (Fig. 2). The Song Da zone rocks are from the Phan Si Pan uplift and Tu Le basin and are correlative with the inner zone of the ELIP. The area is crosscut by the left-lateral ASRR shear zone for over 1000 km from SE Tibet to the South China Sea (Tapponnier *et al*. 1990; Leloup *et al*. 1995; Chung *et al*. 1997). The Phan Si Pan uplift consists mainly of alkaline and sub-alkaline granitoids whereas the Song Da belt consists of picrite, flood basalt and rhyolitic rocks (Hanski *et al*. 2004; Wang *et al*. 2007; Anh *et al*. 2011). The volcanic rocks of the Song Da belt rest on early Permian limestone and are unconformably overlain by Triassic limestone and coal-bearing shale (Anh *et al*. 2011).

Two granitic plutons from the Panxi region of the ELIP were selected for this study (Fig. 3). The peraluminous Yingpanliangzi pluton is located within the city of Panzhihua just south of the Jinsha River and intrudes Proterozoic granitic gneisses (Shellnutt *et al*. 2011a). The pluton is exposed along a dirt road revealing fresh, albeit sporadic outcrops that contain ellipsoidal microgranular enclaves that are more mafic than the host rock. The pluton is known to be younger than ~600 Ma because dykes emanating from the main exposure are observed cutting the Denying (~600 Ma) marble. The sample (GS03-065) dated for this study is located at 26^{o}33’36’’ N, 101^{o}42’53’’ E. The peralkaline Panzhihua granite is located (i.e. 26^{o}34’29’’ N, 101^{o}37’38’’ E) to the west of the Yingpanliangzi pluton and intruded Emeishan flood basalt. The Panzhihua granite is interpreted to be petrogenetically related to the Panzhihua layered gabbroic intrusions which hosts a world-class Fe-Ti-V oxide deposit (Shellnutt & Jahn 2010).

Methods

Zircon U/Pb SHRIMP II ages

Zircon grains were separated using conventional heavy liquid and magnetic techniques, mounted in epoxy, polished, coated with gold, and photographed in transmitted and reflected light to identify grains for analysis. U/Pb isotopic ratios of zircons from sample GS03-065 (i.e. peraluminous granite) were measured using the SHRIMP II at Curtin University of Technology in Perth, Western Australia.

The measured isotopic ratios were reduced off-line using standard techniques (Claoué-Long *et al*. 1995) and the U/Pb ages were normalized to a value of 564 Ma determined by conventional U-Pb analysis of zircon standard CZ3. Common Pb was corrected using the methods of Compston *et al*. (1984). The $^{206}Pb/^{238}U$ and $^{207}Pb/^{235}U$ data were corrected for uncertainties associated with the measurements of the CZ3 standard. The $^{207}Pb/^{206}Pb$ ages given in table 1 are independent of the standard analyses.

Zircon analyses for sample GS03-010 (i.e. peralkaline granite) were measured using the SHRIMP II at Chinese Academy of Geological Sciences, Beijing, China. The measured isotopic ratios were reduced off-line using standard techniques and calibrated to the TEMORA 1 standard which was repeatedly analyzed after every three zircon analyses (Claoué-Long *et al*. 1995; Black *et al*. 2003a, b). Common Pb was corrected using the methods of Compston *et al*. (1984). The $^{206}Pb/^{238}U$ and $^{207}Pb/^{235}U$ data were corrected for uncertainties associated with the measurements of the TEMORA 1 standard. The $^{206}Pb/^{238}U$ and $^{207}Pb/^{235}U$ data are found within table 1.

Zircon Hf LA-ICP-MS values

Hf isotopes were analyzed using a Nu Plasma multi-collector ICP-MS attached to a New Wave UP213 laser-ablation microprobe housed at the Institute of Earth Science, Academia Sinica, Taipei, documented in Lan *et al*. (2009). The analytical procedure follows that described in Griffin *et al*. (2000, 2004). The Hf isotopes were measured on the dated spots of individual zircons to minimize zoning effect but the laser ablation size is 55 µm, slightly larger than that of preexisting spots by the U-Pb dating. Data were normalized to $^{179}Hf/^{177}Hf = 0.7325$, using an exponential correction for mass bias. $^{176}Hf/^{177}Hf$ results of Mud Tank and Harvard zircon standards during analysis of this study are 0.282530 ± 0.000050 (2σ, n = 63) and 0.282314 ± 0.000088 (2σ, n = 22), respectively. $\varepsilon Hf_{(T)}$ values and model ages used in the figures were calculated using the decay constant (1.867×10^{-11} per year) proposed by Söderlund *et al*. (2004). The single stage deplete-mantle model ages (T_{DM1}) and the two-stage model ages (T_{DM2}) are calculated. We assumed that $^{176}Lu/^{177}Hf$ of average continental crust is 0.015 (Griffin *et al*. 2004) for calculation of T_{DM2}. The results are found within table 2.

Results

In situ zircon U/Pb ages

GS03-065 contains zircons with a variety of textures and morphologies. The CL images, Figure 4 show the highly complex internal structure of these zircons. Many zircons exhibit varying degrees of recrystallization. Some have only a thin overgrowth of intermediate U zircon on the rim of crystals, while others have embayments of both high U and low U zircon intergrown within a single crystal (Fig. 4a). The low U region in this grain has a $^{206}Pb/^{238}U$ age of 555 Ma. In figure 4b, the zircon shows three distinct growth zones. An inner low U region is surrounded by oscillatory moderate U zircon and the very centre of the crystal shows a small, higher U region. The oscillatory zoned region has a $^{206}Pb/^{238}U$ age of 671 Ma, while the core age is 701 Ma. There is a progression of recrystallization effects in larger zircons through the two stages shown figure 4. Small, high-U zircons no longer show any oscillatory zoning and have had their ages reset to varying degrees. The lowest $^{206}Pb/^{238}U$ age, 485 Ma, was found in a small, 25 um, high-U (897 ppm) grain. The oldest $^{206}Pb/^{238}U$ age in this population, 787 Ma, was found in a moderate-U (298 ppm) grain which was unzoned. Not all grains have been completely recrystallized or had their ages reset, but there is a strong inverse relationship between U content. Figure 5a gives an overview of the SHRIMP results for GS03-065 plotted on a concordia diagram. Most of analyses plot along a chord with calculated intersections at 264 ± 82 Ma and 806 ± 36 Ma. The upper intersect is the best estimate of the original protolith crystallization age. The lower intercept is identical to that of the mafic-ultramafic and syenite intrusions in the ELIP, which have ages of ~260 Ma and suggests this is the age of the thermal event affecting the recrystallization of the zircons (Shellnutt *et al.*, 2012). The data for this sample is consistent with partial metamorphic/igneous resetting of zircon ages, with the high-U zircons ages being more susceptible to disturbance.

Four inherited zircons were analyzed from sample GS03-010. The crystals are typically between 30 µm to 50 µm and show oscillary zonation and have variable morphologies. The internal structure is less complicated than those from GS03-065 and they are of igneous origin (i.e. Th/U ≤ 1). Figure 5b show the SHRIMP results for GS03-010 plotted on a concordia diagram. Two of the analyses plot along the concordia whereas the other two have suffered U loss. The concordant $^{206}Pb/^{238}U$ ages are 860 ± 7 Ma and 854 ± 8 Ma but the intercept age of all analyses is 848 ± 45 Ma.

In situ zircon Hf isotopes

Hf isotope compositions were analyzed for 18 inherited zircons from the Phan Si Pan granites (table 2). The Neoproterozoic zircons yield Hf isotope compositions in the range of 0.282173 to 0.282299. The zircons have mostly negative $\varepsilon Hf_{(T)}$ values with a few moderately positive values and range between -5.4 and +1.7 which correspond to T_{DM1} model ages between 1.14 Ga to 1.51 Ga. The relatively enriched Hf isotope values indicate that they are either derived from a crustal source or an enriched mantle source.

Discussion

Inherited zircons within plutonic rocks of the Emeishan large igneous province

Shellnutt & Zhou (2007) and Shellnutt *et al*. (2011a) showed that the alumina saturation index (i.e. ASI = Al/Ca+Na+K) offers a simple and relatively robust petrogenetic classification scheme for the Emeishan granitoids. The peralkaline granitoids are interpreted to be derived by fractional crystallization of Emeishan mafic magmas, the metaluminous are interpreted to be derived from mixing of mafic magmas and crustal material (i.e. hybrid) or by partial melting of underplated mafic rocks (i.e. mantle-derived) and the peralumuinous rocks are interpreted to be derived by crustal melting. Therefore the peraluminous Yingpanliangzi, peralkaline Panzhihua and metaluminous Phan Si Pan granitic plutons offer an opportunity to compare the results of inherited zircons from three types of Emeishan silicic rocks that have different petrogenetic histories.

The peraluminous Yingpanliangzi pluton is interpreted to be derived by partial melting of Neoproterozoic granitic rocks (Shellnutt *et al*. 2011a). The upper and lower intercepts ages of the discordia appear to verify that interpretation (Fig. 6a). The pluton has enriched whole rock Sr-Nd (i.e. ISr = 0.7107 to 0.7151; $\varepsilon Nd_{(T)}$ = -3.9 to -4.4), low Nb/U (<6.5) values and high Th/Nb_{PM} (i.e. 9.7 to 16.6) values (Shellnutt *et al*. 2011a). The injection of high temperature magmas into the Yangtze Block is considered to be the primary reason for crustal melting as there are mafic dykes in the same region as well as the Panzhihua layered gabbroic intrusion. The fact that the zircons from the Yingpanliangzi pluton do not form a coherent concordant age coupled with the enriched Sr-Nd isotopes suggests the Neoproterozoic Yangtze crust melted during the emplacement of the ELIP.

Thermodynamic and geochemical modeling indicate that the Panzhihua peralkaline pluton was derived by fractional crystallization of an Emeishan high-Ti basalt and directly related to the neighbouring layered oxide ore-bearing Panzhihua grabbroic intrusion (Shellnutt & Zhou, 2007; Shellnutt & Jahn, 2010; Shellnutt *et al*. 2011b). The *in situ* zircon U/Pb ages show there are Neoproterozoic zircons that have ages of 860 ± 7 Ma and 854 ± 8 Ma with an intercept age of 848 ± 45 Ma. In contrast to the Yingpanliangzi pluton, the Nd isotopes of the Panzhihua pluton are more depleted (i.e. $\varepsilon Nd_{(T)}$ = +2.2 to +2.9) and trace element ratios indicative of mantle-derived rocks (i.e. Th/Nb_{PM} = 1.0 to 1.6; Nb/U = 24.4 to 34.0) rather than crust-derived rocks (Shellnutt & Zhou 2007). The geological relationships (i.e. intruded Emeishan basalt) and mineralogy (i.e. perthitic feldspar) of the Panzhihua pluton suggest that it formed at shallow depth thus the Neoproterozoic zircons are unlikely to originate from the country rock (i.e. basalt). The implication is that the Neoproterozoic zircons were inherited at greater depth before the formation of Panzhihua granitic magma when the parental magma was still basaltic.

Usuki *et al*. (2014) reported the first age dates of silicic rocks from the Phan Si Pan uplift of Northern Vietnam. The rocks range in age from ~252 to ~260 Ma and are geologically correlated with inner zone of the ELIP. The metaluminous to peraluminous Phan Si Pan pluton is ~256 ± 6 Ma and is the only silicic intrusion from northern Vietnam that was found to contain Neoproterozoic zircons. The inherited zircons range in age from 632 Ma to 825 Ma. The Tu Le rhyolite yielded *in situ* zircon U/Pb dates between 252 ± 5 Ma and 262 ± 4 Ma but contained inherited zircons with ages between 708 Ma and 818 Ma. The petrogenetic history of the Phan Si Pan granite and Tu Le rhyolite has not been investigated thoroughly but Tran *et al*. (in preparation) suggest that they are derived from basaltic parental magmas. The Permian zircon $\varepsilon Hf_{(T)}$ values of the granite and rhyolite range between +3.1 and +11.4 which is similar to Emeishan metaluminous granitic rocks that are interpreted to be derived by partial melting of underplated basaltic rocks (Xu *et al*. 2008; Shellnutt *et al*. 2009, 2011a; Usuki *et al*. 2014).

Granitic rocks are not the only rocks that are known to have ancient inherited zircons. Single zircons with ages of 2952 ± 42 Ma, 1927 ± 31 Ma, 1577 ± 26, 1569 ± 29 and 742 ± 13 Ma were found within the Kelang gabbroic intrusion that yielded a mean age of 256 ± 3 Ma (Shellnutt & Wang 2014). The Nd isotopes of the Kelang gabbro are similar to many plutonic rocks in the area and have $\varepsilon Nd_{(T)}$ values of +2.5. The Archean to Neoproterozoic zircon ages correspond to major crust building episodes of the Yangtze Block and indicate that the parental magma interacted with rocks of that age (Qui *et al*. 2000; Zhang *et al*. 2006; Liu *et al*. 2008). The parental magma likely interacted with the lower most part of the crust because basement rocks of Archean age (i.e. Kongling migmatite) are thought to underlie the Proterozoic metasedimentary rocks of the Yangtze Block (Gao *et al*. 1999; Qiu *et al*. 2000;

Zhang *et al*. 2006; Liu *et al*. 2008). In other words, it is unlikely that the Archean zircon was inherited during final stages of emplacement because the surrounding country rocks in the area are Neoproterozoic to Paleozoic.

The Neoproterozoic zircon U/Pb ages indicate that the parental magmas of some Permian silicic and mafic rocks directly interacted with the lower crust of the Yangtze Block however the nature of the magma/country rock interaction remains uncertain. Zircon inheritance is often interpreted to be the result of late stage magma emplacement rather than source origin but the geological relationships of some of the rocks investigated indicates shallow level assimilation is unlikely. The likelihood of an inherited zircon surviving within a melt is related to its original radius, the intensity and duration of the melting event, the degree of Zr undersaturation in the melt, and volume of the local melt reservoir (Watson 1996). Zircons which are likely to survive temperatures $>850^{o}C$ must be > 120 μm whereas zircons < 50 μm will likely be consumed at temperatures of $\sim700^{o}C$ therefore it is possible for original source zircons to survive melting providing they are of sufficient size (Watson 1996). Given the presence of inherited zircons in at least one known mafic intrusion, it is possible that the Neoproterozoic zircons found within some Emeishan magmatic rocks may not only be a consequence of magma/crust interaction but that, in some cases, they indicate the original source was Neoproterozoic in age.

Thermodynamic modeling

Equilibrium partial melt modeling was calculated using the program MELTS on three different Kangdian basaltic rocks as starting compositions in order to determine if they can produce liquid compositions similar to the Emeishan basalts and estimate what the most likely conditions (i.e. temperature, relative oxidation state, initial water content) would have to be in order for melting to occur (Ghiorso & Sack 1995; Smith & Asimow 2005). The initial pressure used for the partial melt modeling is 1.2 GPa (i.e. 12 kbar) which corresponds to the depth (i.e. ~40 km) of the lower crust high seismic velocity layer identified by Xu *et al*. (2004). The initial starting compositions are shown in table 3. The relative oxidation state and initial water content of each model were constrained by trial and error.

The results of the three models are shown figure 6 and can be found within the online supplementary table S1. The best models have an initial water content of 1 wt% and relative oxidation state of FMQ +2. In all cases, the melting curves pass through the total range of Emeishan basalt whole rock data where models EMS1 and EMS2 reproduce the high-Ti basalt compositions and model EMS3 reproduces the low-Ti basalt (Fig. 6). The temperature at which the models predict the composition of the Emeishan basalts is first reached is at 1255^{o}C for models EMS1 and EMS2 and 1275^{o}C for model EM3. The amount of melting required to generate the first liquid composition equal to Emeishan basalt is ~75% for model EMS1, ~70% for model EMS2 and ~50% for model EMS3. Models EMS1 and EMS2 have distinct SiO_2 gaps which form at temperatures of 1215^{o}C (EMS1) and 1190^{o}C (EMS2) which are due to spinel melting and reflects the higher TiO_2 concentration in those models (i.e. TiO_2 > 2.4 wt%) in comparison with EMS3 (i.e. TiO_2 < 1.5 wt%). Therefore, given the modeling parameters used, it is possible that the Kangdian basaltic rocks could produce whole rock compositions similar to the Emeishan basalts.

Plausibility of a Neoproterozoic source for the Emeishan magmatic rocks

The identification of Neoproterozoic zircons within Permian mafic and silicic plutonic rocks and the results of the partial melt modeling indicate that rocks similar in composition to the Kangdian basalts could produce the Emeishan basalts if melted. In order to evaluate the validity of this hypothesis we examine and compare the likely maximum thermal conditions of the ELIP and the isotope compositions of the Neoproterozoic rocks found within the Kangdian/Panxi rift area.

The modeled temperatures required to melt the Kangdian mafic source in order to produce the Emeishan basalts is calculated to be between 1250^{o}C and 1280^{o}C. Estimates of the eruption and mantle potential temperatures (T_p) of the Emeishan ultramafic volcanic rocks were calculated using different techniques by Xu *et al*. (2001), Zhang *et al*. (2006), He *et al*. (2010) and Ali *et al*. (2010). Xu *et al*. (2001) used REE inversion and estimated the mantle potential temperatures to be > 1550^{o}C whereas Zhang *et al*. (2006) calculated mantle potential temperatures between 1630^{o}C and 1690^{o}C. He *et al*. (2010) and Ali *et al*. (2010) calculated eruption temperatures of ~1440^{o}C and mantle potential temperatures between ~1540^{o}C and ~1610^{o}C using PRIMELT2 assuming initial MgO values of the picrites to be ≥20%. The wide range of mantle potential temperature may be related to differences in the thermodynamic assumptions for each calculation method but all results reveal temperatures >1540^{o}C which are ~150^{o}C above the Tp estimates of primitive MORB values and are supportive of a high temperature regime (Campbell 2005; Ali *et al*. 2010). Additionally, the eruption temperature estimates of the picrites (i.e. ~1440^{o}C) are greater than the temperatures required to induce melting of the underplated mafic rocks and thus the thermal requirements of the MELTS models is plausible.

The Emeishan basalts have $\varepsilon Nd_{(T)}$ values ranging from -14.2 to +6.4 with a mean value of +0.1 ± 0.5 2σ (Fig, 6). The Sr, Os and Pb isotopes also show a wide range in composition (i.e. I_{Sr} = 0.7040 to 0.7132; γOs = -5 to +11 and $^{206}Pb/^{204}PbPb_1$ = 17.9 to 19.7). In comparison, albeit a smaller database, the ultramafic volcanic rock have a higher average $\varepsilon Nd_{(T)}$ value (i.e. $\varepsilon Nd_{(T)}$ = +3.0 ± 1.4 2σ), including the single highest reported value of +7.8, but there is also a wide (i.e. $\varepsilon Nd_{(T)}$ = -7.8 to +7.8) range (Kamenetsky *et al*. 2012). The range in composition of the Emeishan basalts makes it difficult to distinguish between a specific source (i.e. SCLM or sublithospheric source or both) or process (i.e. crustal assimilation or mixing between an enriched component and mantle source) to explain the isotope variability (Shellnutt 2014).

The Nd-Hf isotopes of the Kangdian basalts and mafic dykes are moderately depleted (i.e. $\varepsilon Nd_{(T)}$ = +5.0 to +6.0, $\varepsilon Hf_{(T)}$ = +7.9 to +17.4) although some differentiated basalts and trachyandesite have more enriched values (i.e. $\varepsilon Nd_{(T)}$ = +1.4 to +2.4, $\varepsilon Hf_{(T)}$ = +4.3 to +8.0) which are attributed to crustal contamination (Li *et al*. 2002, 2005; Lin *et al*. 2007). Zhao *et al*. (2008) describe Neoproterozoic A- and I-type granites with $\varepsilon Nd_{(T)}$ values of +1 and zircon $\varepsilon Hf_{(T)}$ values of +5 to +9 whereas Zhao & Zhou (2007) describe a group of slightly younger (i.e. ~750 Ma) mafic intrusions in southern Sichuan (near Panzhihua) that are interpreted to be derived by partial melting of a garnet-bearing metasomatised upper mantle. The gabbros have I_{Sr} (i.e. I_{Sr} = 0.7040 to 0.7070) and $\varepsilon Nd_{(T)}$ (i.e. $\varepsilon Nd_{(T)}$ = -0.6 to -1.7) values that are indicative of a more enriched mantle source. The isotopic range of the Emeishan basalts, in particular Nd isotopes, overlaps with the Neoproterozoic rocks. Furthermore the Hf isotopes from the inherited zircons from NW Vietnam have $\varepsilon Hf_{(T)}$ values are between -5.4 and +1.7 which would equal $\varepsilon Nd_{(T)}$ values of -6.3 to -1.1 (e.g. $\varepsilon Hf = 1.36\varepsilon Nd + 3.19$) and fall within the range of Emeishan basalt and similar to the 750 Ma mafic intrusions. Therefore it is possible that the Neoproterozoic mafic rocks, if melted, could produce the isotopic range observed within the Emeishan mafic and some silicic rocks.

An alternative model for the genesis of the Emeishan basalts

Many models for the petrogenesis of the ELIP invoke a mantle plume model to explain the presence of ultramafic rocks and voluminous flood basalts (Xu *et al*. 2001, 2004; Xiao *et al*. 2004; Song *et al*. 2004; Ali *et al*. 2005, 2010; Fan *et al*. 2008; Shellnutt 2014). Isotope enrichment and variability in some trace element ratios (e.g. Th/Nb_{PM}, Nb/U) of the Emeishan basalts is interpreted to be related to crustal contamination with either a heterogeneous mantle source or a two mantle source (i.e. SCLM plus sub-lithospheric mantle). However we suggest that it is possible that some mafic and silicic ELIP-related magmatic rocks can be derived from Neoproterozoic lower crust rocks. The temperature estimates of the ultramafic volcanic rocks is high enough to induce melting of mafic underplated Neoproterozoic rocks and produce some ‘second’ generation magmas with a large range of isotopic compositions without necessarily showing evidence of sialic crustal assimilation. Furthermore it is possible that some of the underplated Neoproterozoic rocks chemically equilibrated with older Yangtze Block rocks and therefore could have more enriched isotopic compositions if melted. For example, there are some Emeishan basalts that have enriched Nd isotope signatures (i.e. $\varepsilon Nd_{(T)} > -2$) but do not show strong evidence of crustal assimilation (i.e. $Th/Nb_{PM} < 2.5$, $Nb/U > 25$) (Fig. 7).

The high seismic velocity layers in the lower crust of the Yangtze Block could represent pure Emeishan material, pure Neoproterozoic material or a mixture of both but none of these interpretations can be dismissed outright because there are no age constraints on the seismic layers. The MELTS models, thermal estimates of the Emeishan ultramafic volcanic rocks and Nd-Hf isotope range of the Kangdian rocks indicate that it is possible to generate derivative liquid compositions that resemble Emeishan basalts and thus it is plausible that mafic Neoproterozoic rocks could be the source of some Emeishan mafic or silicic rocks and that they are a consequence of lower crustal recycling indirectly related to a Neoproterozoic mantle plume rather than a direct lineage to the Permian mantle plume (Fig. 8). Although the Permian mantle plume model is a preferred interpretation for the genesis of the Emeishan ultramafic volcanic rocks and probably most basalts but the possibility that partial melting of mafic Neoproterozoic lower crustal rocks could produce some of the mafic and silicic ELIP magmatic rocks cannot be easily disproved. The results of this study imply that, in some cases, mantle-plume derived large igneous provinces contribute to crustal recycling as well as juvenile crust formation.

Conclusions

Late Permian mafic and silicic plutonic rocks associated with the Emeishan large igneous province have inherited zircons which yield Neoproterozoic U/Pb ages. The Neoproterozoic zircons indicate that at least some of the ELIP magmatic rocks have evidence for direct interaction with the lower crustal rocks of the Yangtze Block. The precise nature of the magma/crust interaction is uncertain as the zircons may have been assimilated during emplacement or they could represent inheritance from the original source rocks. Thermodynamic modeling indicates that compositions similar to the Emeishan flood basalts can be produced by partial melting of the Neoproterozoic Kangdian basalt at conditions equal to a pressure of 1.2 GPa, water content of ~1 wt% and fO_2 of FMQ +2. The identification of high velocity seismic layers in the lower crust of the Yangtze Block, interpreted as being related to the Emeishan mantle plume, may, in fact, represent underplated mafic to ultramafic rocks from the Neoproterozoic magmatic event or a mixture of Neoproterozoic and Permian magmatic rocks. The presence of Late Permian ultramafic volcanic rock with estimated eruption temperatures >1400^{o}C would be sufficient to induce partial melting (i.e. 1250^{o}C to 1280^{o}C) of the underplated mafic rocks to the extent indicated by the partial melt models. Therefore, it is possible, that some Emeishan flood basalts and other magmatic rocks were formed by juvenile crustal recycling induced by a high temperature regime attributed to the Emeishan mantle plume.

J.G.S. would like to acknowledge the support of the National Science Council of Taiwan through grant NSC 102-2628-M-003-001-MY4.

References

Ali, J.R., Thompson, G.M., Zhou, M.-F. & Song, X.Y. 2005. Emeishan large igneous province, SW China. *Lithos*, **79**, 475-489.

Ali, J.R., Fitton, J.G. & Herzberg, C. 2010. Emeishan large igneous province (SW China) and the mantle-plume up-doming hypothesis. *Journal of the Geological Society*, **167**, 953-959.

Anh, T.T., Hoa, T.T., Lan, C.Y., Chung, S.-L., Lo, C.H., Wang, P.L. & Mertzman, S. 2004. Mesozoic bimodal alkaline magmatism in Tu Le basin, North Vietnam: Constraints from geochemical and isotopic significances. *Journal of Geology, Series B*, **24**, 1-9.

ANH, T.V., PANG, K.N., CHUNG, S.-L., LIN, H.M., HOA, T.T., ANH, T.T. & YANG, H.J. 2011. The Song Da magmatic suite revisited: A petrologic, geochemical and Sr–Nd isotopic study on picrites, flood basalts and silicic volcanic rocks. *Journal of Asian Earth Sciences*, **42**, 1341-1355.

BLACK, L.P., KAMO S.L., ALLEN, C.M., ALEINIKOFF, J.N., DAVIS, D.W., KORSCH, R.J. & FOUDOULIS, C. 2003a. TEMORA 1: a new zircon standard for Phanerozoic U-Pb geochronology. *Chemical Geology*, **200**, 155-170.

BLACK, L.P., KAMO, S.L., WILLIAMS, I.S., MUNDIL, R., DAVIS, D. W., KORSCH, R.J. & FOUDOULIS, C. 2003b. The application of SHRIMP to Phanerozoic geochronology; a critical appraisal of four zircon standards. *Chemical Geology*, **200**, 171-188.

CAMPBELL, I.H. 2007. Testing the plume theory. *Chemical Geology*, **241**, 153-176.

CAMPBELL, I.H. 2005. Large igneous provinces and the mantle plume hypothesis. *Elements*, **1**, 265-269.

CHEN, J., YANG, X., XIAO, L. & HE, Q. 2010. Coupling of basaltic magma evolution and lithospheric seismic structure in the Emeishan large igneous province: MELTS modeling constraints. *Lithos*, **119**, 61-74.

CHUNG, S.-L. & JAHN, B.-M. 1995. Plume-lithosphere interaction in generation of the Emeishan flood basalts at the Permian-Triassic boundary. *Geology*, **23**, 889-892.

CHUNG, S.-L., LEE, T.Y., LO, C.H., WANG, P.L., CHEN, C.Y., NGUYEN, T.Y., HOA, T.T. & WU, G. 1997. Intraplate extension prior to continental extrusion along the Ailao Shan-Red River shear zone. *Geology*, **25**, 311-314.

CLAOUE-LONG, J.C., COMPSTON, W., ROBERTS, J. & FANNING, M. 1995. Two Carboniferous ages: a comparison of SHRIMP zircon dating with conventional zircon ages and $^{40}Ar/^{39}Ar$ analysis. *Geochronology Time Scales and Global Stratigraphic Correlation, SEPM Special Publication*, **54**, 3-21.

Compston, W., Williams, I.S. & Meyer, C. 1984. U-Pb geochronology of zircons from Lunar breccia 73217 using a sensitive high mass-resolution ion microprobe. *Journal of Geophysical Research*, **89**, 525-534.

Dao, D.T., & Huynh, T. 1995. Magmatic formations of Vietnam. Vietnamese Geological Survey (in Vietnamese).

Dovjikov A.E. 1965. Geology of North Vietnam. Publishing House Sciences and Technics, 668 pp. (in Vietnamese).

Fan, W., Zhang, C., Wang, Y., Guo, F. & Peng, T. 2008. Geochronology and geochemistry of Permian basalts in western Guangxi Province, southwest China: evidence for plume-lithosphere interaction. *Lithos*, **102**, 218-236.

Gao, S., Ling, W.L., Qiu, Y.M., Zhou, L., Hartmann, G., Simon, K. 1999. Contrasting geochemical and Sm-Nd isotopic compositions of Archean metasediments from the Kongling high-grade terrane of the Yangtze craton: evidence for cratonic evolution and redistribution of REE during crustal anatomies. *Geochimica et Cosmochimica Acta*, **63**, 2071-2088.

Ghiorso, M.S. & Sack, R.O. 1995. Chemical mass transfer in magmatic processes IV. A revised and internally consistent thermodynamic model for the interpolation and extrapolation of liquid-solid equilibria in magmatic systems at elevated temperatures and pressures. *Contributions to Mineralogy and Petrology*, **119**, 197-212.

Griffin, W.L., Pearson, N.J., Belousova, E.A., Jackson, S.E., O'Reilly, S.Y., van Achterberg, E. & Shee, S.R. 2000. The Hf-isotope composition of cratonic mantle: LAM-MC-ICPMS analysis of zircon megacrysts in kimberlites. *Geochimica et Cosmochimica Acta*, **64**, 133–147.

Griffin, W.L., Belousova, E.A., Shee, S.R., Pearson, N.J. & O'Reilly, S.Y. 2004. Archean crustal evolution in the northern Yilgarn Craton: U–Pb and Hf-isotope evidence from detrital zircons. *Precambrian Research*, **131**, 231–282.

Hanski, E., Walker, R.J., Huhma, H., Polyakov, G.V., Balykin, P.A., Hoa, T.T. & Phuong, N.T. 2004. Origin of the Permian-Triassic komatiites, northwestern Vietnam. *Contributions to Mineralogy and Petrology*, **147**, 453-469.

He, B., Xu, Y.-G., Chung, S.-L., Xiao, L. & Wang, Y. 2003. Sedimentary evidence for a rapid, kilometer-scale crustal doming prior to the eruption of the Emeishan flood basalts. *Earth and Planetary Science Letters*, **213**, 391-405.

He, Q., Xiao, L., Balta, B., Gao, R. & Chen, J. 2010. Variety and complexity of the Late-Permian Emeishan basalts: reappraisal of plume-lithosphere interaction processes. *Lithos*, **119**, 91-107.

Hou, Z.Q., Lu, J.R. & Lin, S.Z. 2006. Heterogeneity of a plume axis: bulk-rock geochemical evidence from picrites and basalts in the Emei large igneous province, southwest China. *International Geology Review*, **48**, 1087-1112.

Kamenetsky, V.S., Chung, S.-L., Kamenetsky, M.B. & Kuzmin, D.V. 2012. Picrites from the Emeishan large igneous province, SW China: a compositional continuum in primitive magmas and their respective mantle sources. *Journal of Petrology*, **53**, 2095-2113.

Lan, C.Y., Usuki, T., Wang, K.L., Yui, T.F., Okamoto, K., Lee, Y.H., Hirata, T., Kon, Y., Orihashi, Y., Liou, J.G. & Lee, C.S. 2009. Detrital zircon evidence for the antiquity of Taiwan. *Geosciences Journal*, **13**, 233–243.

Lan, C.Y., Chung, S.L., Lo, C.H., Lee, T.Y., Wang, P.L., Li, H. & Dinh, V.T. 2001. First evidence for Archean continental crust in northern Vietnam and its implications for crustal and tectonic evolution in Southeast Asia. *Geology*, **29**, 219-222.

Leloup, P.H., Lacassin, R., Tapponnier, P., Schärer, U., Zhong, D., Liu, X., Zhang, L.S., Ji, S.C. & Phan, T.T. 1995. The Ailao Shan-Red River shear zone (Yunnan, China), Tertiary transform boundary of Indochina. *Tectonophysics*, **251**, 3-84.

Li, X.-H., Li, Z.-X., Sinclair, J.A., Li, W.-X. & Carter, G. 2006. Revisiting the “Yanbian Terrane”: implications for Neoproterozoic tectonic evolution of the western Yangtze block, South China. *Precambrian Research*, **151**, 14-30.

Li, X., Qi, C., Liu, Y., Liang, X., Tu, X., Xie, L. & Yang, Y. 2005. Petrogenesis of the Neoproterozoic bimodal volcanic rocks along the western margin of the Yangtze block: new constraints from Hf isotopes and Fe/Mn ratios. *Chinese Science Bulletin*, **50**, 2481-2486.

Li, X.-H., Li, Z.-X., Zhou, H., Liu, Y. & Kinny, P.D. 2002. U-Pb zircon geochronology, geochemistry and Nd isotopic study of Neoproterozoic bimodal volcanic rocks in the Kangdian rift of South China: implications for the initial rifting of Rodinia. *Precambrian Research*, **113**, 135-154.

Li, Z.X., Li, X.H., Kinny, P.D. & Wang, J. 1999. The breakup of Rodinia: did it start with a mantle plume beneath South China? *Earth and Planetary Science Letters*, **173**, 171-181.

Lin, G., Li, X. & Li, W. 2007. SHRIMP U-Pb zircon age, geochemistry and Nd-Hf isotope of Neoproterozoic mafic dyke swarms in western Sichuan: petrogenesis and tectonic significance. *Science in China: Earth Sciences*, **50**, 1-16.

Ma, Y.X., Zhou, R.S., Wan, Y.W., Liu, F., Qiu, Y.D. & Wang H.F. 1999. Geology of Panzhihua City area (Map G-47-60-A). Chengdu University of Science and Technology, 1: 50000.

Nam, T.N. 2001. Ages of the Ca Vinh and Xom Giau complexes: First reliable evidence from SHRIMP U-Pb zircon dating. *Geology Series A*, **262**, 1-11 (in Vietnamese).

Nam, T.N. Toruimi M., Sano Y., Terada K. & Thang T.T. 2003. 2.9, 2.36 and 1.96 Ga zircon in orthogneiss south of Red River shear zone in Vietnam: evidence from SHRIMP U-Pb dating and tectonothermal implications. *Journal of Asian Earth Sciences*, **21**, 743-753.

Qiu, Y.M., Gao, S., McNaughton, N.J., Groves, D.I., Ling, W. 2000. First evidence of > 3.2 Ga continental crust in the Yangtze craton of south China and its implications for Archean crustal evolution and Phanerozoic tectonics. *Geology*, **28**, 11-14.

Rudnick, R.L. & Gao, S., 2003. Composition of the continental crust. *In*: Rudnick, R.L. (ed) *The Crust*. Treatise on Geochemistry, **3**, 1-64.

Shellnutt, J.G. 2014. The Emeishan large igneous province: a synthesis. *Geoscience Frontiers*, **5**, 369-394.

Shellnutt, J.G. & Wang, K.-L. 2014. An ultramafic parental magma for a low Si-Al, high Ti-Fe gabbro in the Panxi region of the Emeishan large igneous province, SW China. *Journal of Asian Earth Sciences*, **79**, 329-344.

Shellnutt, J.G., Denyszyn, S. & Mundil, R. 2012. Precise age determination of mafic and felsic intrusive rocks from the Permian Emeishan large igneous province (SW China). *Gondwana Research*, **22**, 118-126.

Shellnutt, J.G. & Jahn, B.-M. 2011. Origin of Late Permian Emeishan basaltic rocks from the Panxi region (SW China): implications for the Ti-classification and spatial-compositional distribution of the Emeishan basalts. *Journal of Volcanology and Geothermal Research*, **199**, 85-95.

Shellnutt, J.G., Jahn, B.-M. & Zhou, M.-F. 2011a. Crustal-derived granites in the Panzhihua region, SW China: implications for felsic magmatism in the Emeishan large igneous province. *Lithos*, **123**, 145-157.

Shellnutt, J.G., Wang, K.-L., Zellmer, G.F., Iizuka, Y., Jahn, B.-M., Pang, K.-N., Qi, L. & Zhou, M.-F. 2011b. Three Fe-Ti oxide ore-bearing gabbro-granitoid complexes in the Panxi region of the Emeishan large igneous province, SW China. *American Journal of Science*, **311**, 773-812.

Shellnutt, J.G. & Jahn, B.-M. 2010. Formation of the Late Permian Panzhihua plutonic-hypabyssal-volcanic igneous complex: implications for the genesis of Fe-Ti oxide deposits and A-type granites of SW China. *Earth and Planetary Science Letters*, **289**, 509-519.

Shellnutt, J.G. & Zhou, M.-F. 2007. Permian peralkaline, peraluminous and metaluminous A-type granites in the Panxi district, SW China: their relationship to the Emeishan mantle plume. *Chemical Geology*, **243**, 286-316.

SMITH, P.M. & ASIMOW, P.D. 2005. Adiabat_1ph: a new public front-end to the MELTS, pMELTS, and pHMELTS models. *Geochemistry, Geophysics Geosytems*, **6**, Q02004, doi: 10.1029/2004GC000816.

SÖDERLUND, U., PATCHETT, P.J., VERVOORT, J.D. & ISACHSEN, C.E. 2004. The ^{176}Lu decay constant determined by Lu–Hf and U–Pb isotope systematics of Precambrian mafic intrusions. *Earth and Planetary Science Letters*, **219**, 311–324.

SONG, X.Y., QI, H.-W., ROBINSON, P.T., ZHOU, M.-F., CAO, Z.-M. & CHEN, L.-M. 2008a. Melting of the subcontinental lithospheric mantle by the Emeishan mantle plume; evidence from the basal alkaline basalts in Dongchuan, Yunnan, southwestern China. *Lithos*, **100**, 93-111.

SONG, X.-Y., ZHOU, M.-F., TAO, Y. & XIAO, J.-F. 2008b. Controls on the metal compositions of magmatic sulfide deposits in the Emeishan large igneous province, SW China. *Chemical Geology*, **253**, 38-49.

SONG, X.-Y., ZHOU, M.-F., CAO, Z.-M. & ROBINSON, P. 2004. Late Permian rifting of the South China craton caused by the Emeishan mantle plume? *Journal of Geological Society*, **161**, 773-781.

SONG, X.-Y., ZHOU, M.-F., HOU, Z.-Q., CAO, Z.-M., WANG, Y.-L. & LI, Y. 2001. Geochemical constraints on the mantle source of the upper Permian Emeishan continental flood basalts, southwestern China. *International Geology Review*, **43**, 213-225.

TAPPONNIER P., LACASSIN R., LELOUP, P.H., SCHARER, U., ZHONG, D., LIU X., JI, S., ZHANG, L. & ZHONG J. 1990. The Ailao Shan/Red River metamorphic belt: Tertiary left-lateral shear between Indochina and South China. *Nature*, **343**, 432-437.

TRAN, D.L. & NGUYEN, X.B. 1988. Geological Map of Vietnam, scale 1: 500.000. Vietnam General Department of Geology and Mining.

TRAN, V.T. 1977. Geology of Vietnam. North part. Explanation to geological map of Vietnam, North part, scale 1: 1,000,000. Publishing House Sciences and Technics, 355 pp. (in Vietnamese).

USUKI, T., LAN, C.-Y., HOA, T.T., DUNG, P.T., WANG, K.-L., SHELLNUTT, J.G. & CHUNG, S.-L. 2014. Zircon U-Pb ages and Hf isotopic compositions of alkaline silicic magmatic rocks in the Phan Si Pan-

Tu Le region, northern Vietnam: identification of a displacement western extension of the Emeishan large igneous province. *Journal of Asian Earth Sciences*, doi: 10.1016/j.jseaes.2014.10.016.

WANG, C.Y., ZHOU, M.-F. & QI, L. 2011. Chalcophile element geochemistry and petrogenesis of high-Ti and low-Ti magmas in the Permian Emeishan large igneous province, SW China. *Contributions to Mineralogy and Petrology*, **161**, 237-254.

WANG, C.Y., ZHOU, M.F. & QI, L. 2007. Permian flood basalts and mafic intrusions in the Jinping (SW China)–Song Da (northern Vietnam) district: Mantle sources, crustal contamination and sulfide segregation. *Chemical Geology*, **243**, 317-343.

WANG, Q., WYMAN, D.A., LI, Z.-X., BAO, Z.-W., ZHAO, Z.-H., WANG, Y.-X., JIAN, P., YANG, Y.-H. & CHEN, L.-L. 2010. Petrology, geochronology and geochemistry of ca. 780 Ma A-type granites in South China: petrogenesis and implications for crustal growth during the breakup of the supercontinent Rodinia. *Precambrian Research*, **178**, 185-208.

WANG, X.-C., LI, X.-H., LI, W.-X. & LI, Z.-X. 2009. Variable involvements of mantle plumes in the genesis of mid-Neoproterozoic basaltic rocks in South China: a review. *Gondwana Research*, **15**, 381-395.

WATSON, E.B. 1996. Dissolution, growth and survival of zircons during crustal fusion: kinetic principals, geological models and implications for isotopic inheritance. *Transactions of the Royal Society of Edinburgh*, **87**, 43-56.

WIEDENBECK, M., ALLE, P., CORFU, F., GRIFFIN, W.L., MEIER, M., OBERLI, F., VON QUADT, A., RODDICK, J.C. & SPIEGEL, W. 1995. Three natural zircon standards for U-Th-Pb, Lu-Hf, trace element and REE analyses. *Geostandards and Geoanalytical Research*, **19**, 1-23.

XIAO, L., XU, Y.G., MEI, H.J., ZHENG, Y.F., HE, B. & PIRAJNO, F. 2004. Distinct mantle sources of low-Ti and high-Ti basalts from the western Emeishan large igneous province, SW China: implications for plume–lithosphere interaction. *Earth and Planetary Science Letters*, **228**, 525–546.

Xu, Y.-G. & He, B. 2007. Thick and high velocity crust in Emeishan large igneous province, SW China: Evidence for crustal growth by magmatic underplating/intraplating. *In*: Foulger, G.R. & Jurdy, D.M. (eds) *Plates, Plumes and Planetary Processes*. Geological Society of America Special Paper, **430**, 841-858.

Xu, Y.G., He, B., Chung, S.L., Menzies, M. & Frey, F.A. 2004. Geologic, geochemical, and geophysical consequences of plume involvement in the Emeishan flood-basalt province. *Geology*, **32**, 917-920.

Xu, Y., Chung, S.L., Jahn, B.M. & Wu, G. 2001. Petrologic and geochemical constraints on the petrogenesis of Permian-Triassic Emeishan flood basalts in southwestern China. *Lithos*, **58**, 145-168.

Zhang, Z., Mahoney, J.J., Mao, J. & Wang, F. 2006. Geochemistry of Picritic and Associated Basalt Flows of the Western Emeishan Flood Basalt Province, China. *Journal of Petrology*, **47**, 1997-2019.

Zhao, J.-H. & Zhou, M.-F. 2007. Geochemistry of Neoproterozoic mafic intrusions in the Panzhihua district (Sichuan Province, SW China): Implications for subduction-related metasomatism in the upper mantle. *Precambrian Research*, **152**, 27-47.

Zhao, X.-F., Zhou, M.-F., Li, J.-W. & Wu, F.-Y. 2008. Association of Neoproterozoic A- and I-type granites in South China: implications for generation of A-type granites in a subduction-related environment. *Chemical Geology*, **257**, 1-15.

Zhou, J., Wang, X., Qiu, J. & Gao, J. 2004. Geochemistry of Meso- and Neoproterozoic mafic-ultramafic rocks from northern Guangxi, China: arc or plume magmatism. *Geochemical Journal*, **38**, 139-152.

Zhou, M.-F., Arndt, N.T., Malpas, J., Wang, C.Y. & Kennedy, A.K. 2008. Two magma series and associated ore deposit types in the Permian Emeishan large igneous province, SW China. *Lithos*, **103**, 352-368.

Zhou, M.-F., Yan, D.P., Kennedy, A.K. Li, Y. & Ding, J. 2002a. SHRIMP U-Pb zircon geochronological and geochemical evidence for Neoproterozoic arc-magmatism along the western margin of the Yangtze block, South China. *Earth and Planetary Science Letters*, **196**, 51-67.

ZHOU, M.-F., KENNEDY, A.K., SUN, M., MALPAS, J. & LESHER, C.M. 2002a. Neo-proterozoic arc-related mafic intrusions along the northern margin of South China: implications for accretion of Rodinia. *Journal of Geology*, **110**, 611-618.

Figure Captions

Fig. 1. (a) Distribution of the Emeishan large igneous province showing the concentric zones (dashed red lines) and locations of the Panxi intrusions and Song Da intrusion. (b) Seismic P-wave velocity (km/s) structure of the lower crust and upper mantle beneath the western Yangtze Block from Lijiang (A) to Zhehai (B) (modified from Xu *et al*. 2004).

Fig. 2. Simplified geological map of NW Vietnam (modified from Usuki *et al*., 2014).

Fig. 3. Sample geological map of the Panzhihua region showing the locations of samples GS03-065 (Yingpanliangzi granite) and GS03-010 (Panzhihua granite). Modified from Ma *et al.* (1999).

Fig. 4. Cathodoluminescence images of (a) one zircon showing highly complex internal structure. Zone 1 is a low U region whereas zone 2 is a high U region. (b) Multiple growth zones with a low U core.

Fig. 5. Concordia diagrams of the (a) Yingpanliangzi pluton and the (b) Panzhihua peralkaline granite.

Fig. 6. Results of equilibrium partial melt modeling of the Kangdian mafic rocks. All models rocks were calculated at a relative oxidation state of FMQ +2, pressure of 1.2 GPa and water content of 1 wt%. Source rock compositions can be found in table 3. All modeled results and Emeishan basalt data normalized to 100%. Emeishan basalt data compiled in Shellnutt & Jahn (2011).

Fig. 7. (a) $\varepsilon Nd_{(T)}$ vs. Nb/U ratio of the high-Ti and low-Ti Emeishan flood basalts, Emeishan ultramafic volcanic rocks and Neoproterozoic mafic rocks. (b) $\varepsilon Nd_{(T)}$ vs. Th/Nb_{PM} ratio of the high-Ti and low-Ti Emeishan flood basalts, Emeishan ultramafic volcanic rocks and Neoproterozoic mafic rocks. The Th/Nb ratio is normalized to primitive mantle of Sun & McDonough (1989). The values of average

lower crust and upper crust from Rudnick and Gao (2003). Emeishan compiled in Shellnutt & Jahn (2011) and Kamenetsky *et al*. (2012). Data for the Kangdian basalts and mafic intrusions from Li *et al*. (2002, 2006, 2007) and Zhao & Zhou (2007).

Fig. 8. Conceptual model of the lower crust origin of some Emeishan magmatic rocks.

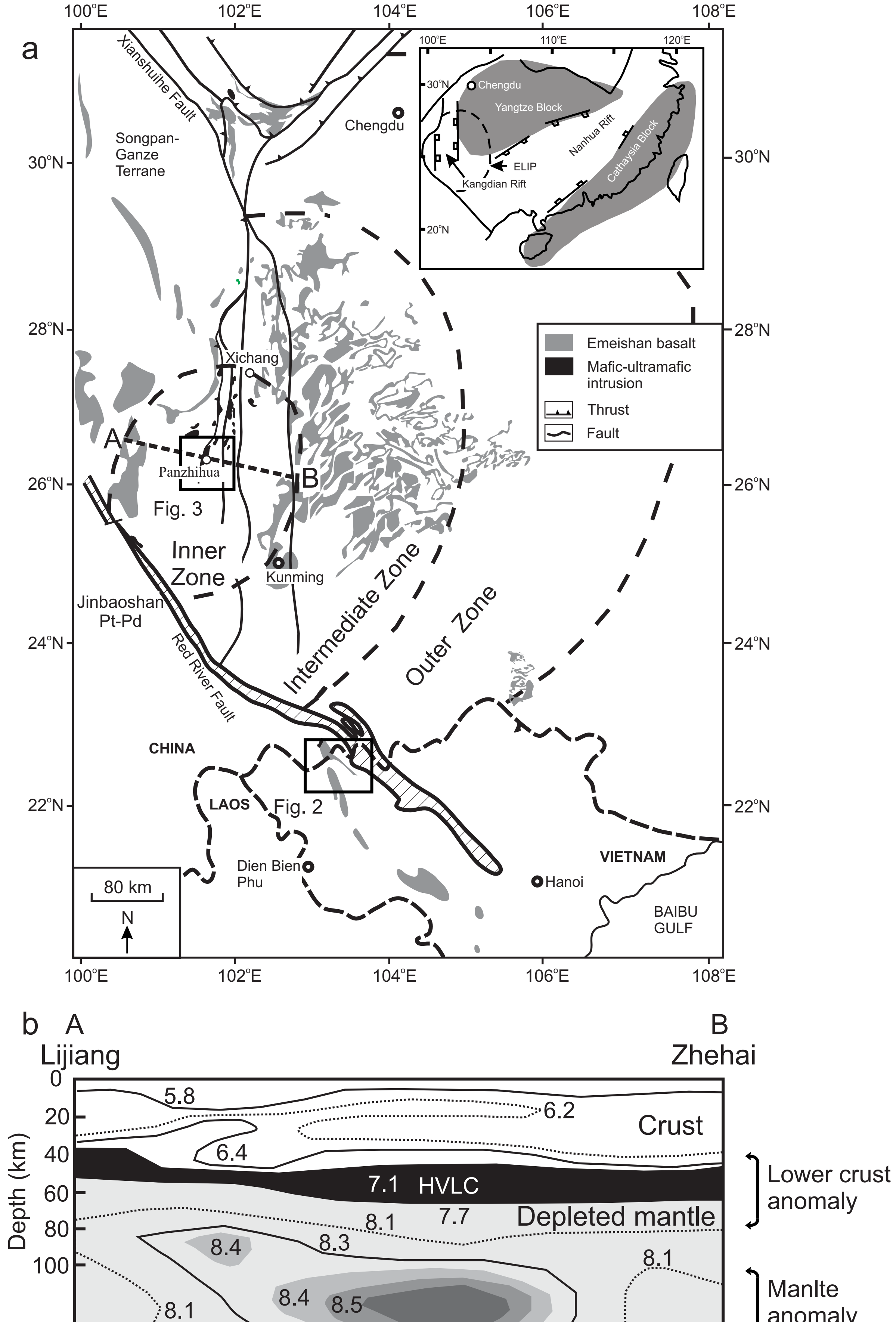

a
100°E
102°E
104°E
106°E
108°E
30°N
28°N
26°N
24°N
22°N
Xianshuihe Fault
Songpan-Ganze Terrane
Chengdu
Yangtze Block
Nanhua Rift
Cathaysia Block
ELIP
Kangdian Rift
Emeishan basalt
Mafic-ultramafic intrusion
Thrust
Fault
Xichang
A
B
Panzhihua
Fig. 3
Inner Zone
Kunming
Intermediate Zone
Outer Zone
Jinbaoshan Pt-Pd
Red River Fault
CHINA
LAOS
Fig. 2
Dien Bien Phu
Hanoi
VIETNAM
BAIBU GULF
80 km
N
b A
Lijiang
B
Zhehai
Depth (km)
5.8
6.2
Crust
6.4
7.1 HVLC
8.1
7.7
Depleted mantle
8.4
8.3
8.1
8.4
8.5
8.1
Lower crust anomaly
Manlte anomaly

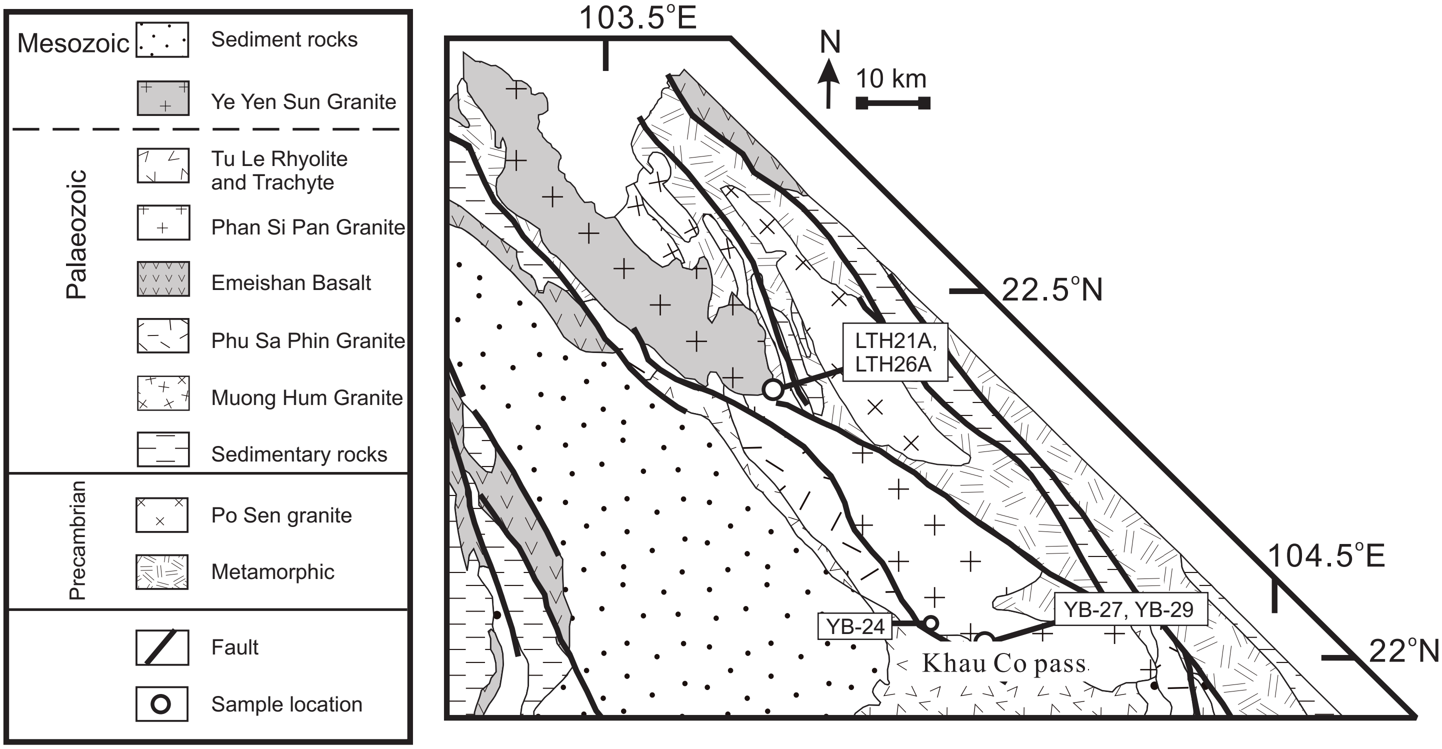
Mesozoic
Sediment rocks
Ye Yen Sun Granite
Palaeozoic
Tu Le Rhyolite and Trachyte
Phan Si Pan Granite
Emeishan Basalt
Phu Sa Phin Granite
Muong Hum Granite
Sedimentary rocks
Precambrian
Po Sen granite
Metamorphic
Fault
Sample location
103.5°E
N
10 km
22.5°N
LTH21A, LTH26A
104.5°E
22°N
YB-24
YB-27, YB-29
Khau Co pass

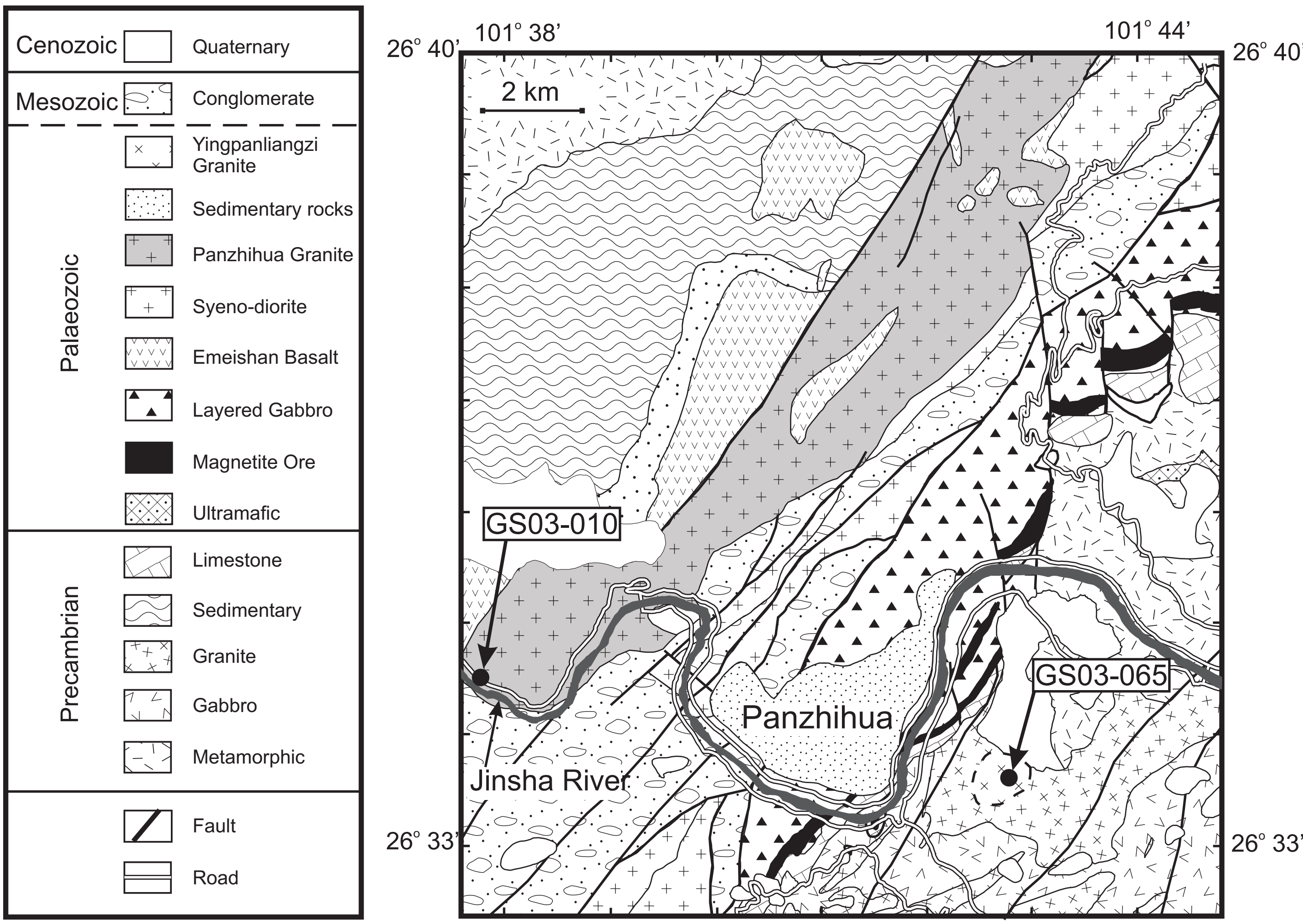
Cenozoic
Quaternary
Mesozoic
Conglomerate
Palaeozoic
Yingpanliangzi Granite
Sedimentary rocks
Panzhihua Granite
Syeno-diorite
Emeishan Basalt
Layered Gabbro
Magnetite Ore
Ultramafic
Precambrian
Limestone
Sedimentary
Granite
Gabbro
Metamorphic
Fault
Road
101° 38’
101° 44’
26° 40’
26° 40’
2 km
GS03-010
GS03-065
Panzhihua
Jinsha River
26° 33’
26° 33’
101° 38’
101° 45’

a

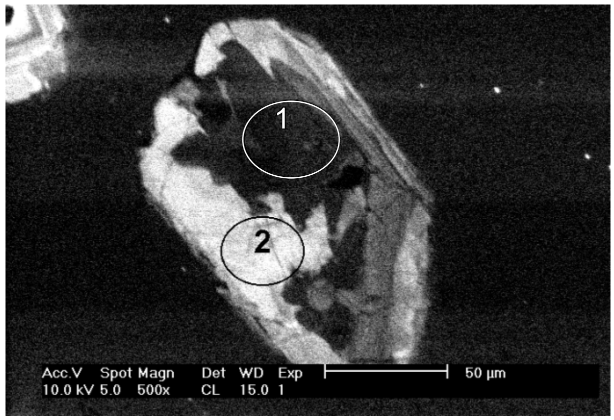
1
2
Acc.V Spot Magn Det WD Exp
50 µm
10.0 kV 5.0 500x CL 15.0 1

b

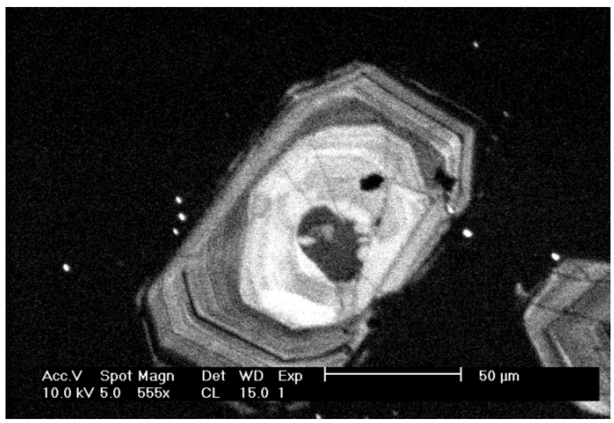
Acc.V Spot Magn Det WD Exp
50 µm
10.0 kV 5.0 555x CL 15.0 1

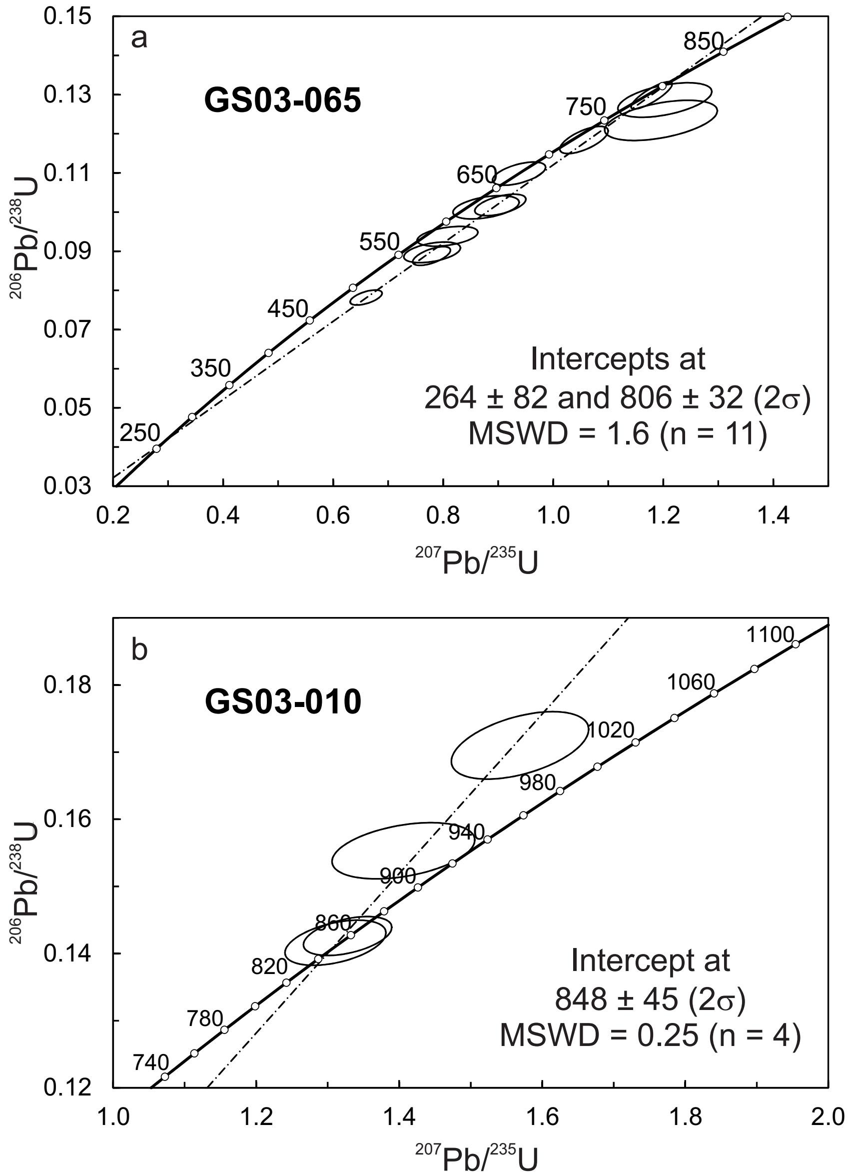
a
GS03-065
Intercepts at
264 ± 82 and 806 ± 32 (2σ)
MSWD = 1.6 (n = 11)
250
350
450
550
650
750
850
0.15
0.13
0.11
0.09
0.07
0.05
0.03
0.2
0.4
0.6
0.8
1.0
1.2
1.4
206Pb/238U
207Pb/235U
b
GS03-010
Intercept at
848 ± 45 (2σ)
MSWD = 0.25 (n = 4)
740
780
820
860
900
940
980
1020
1060
1100
0.18
0.16
0.14
0.12
1.0
1.2
1.4
1.6
1.8
2.0
206Pb/238U
207Pb/235U

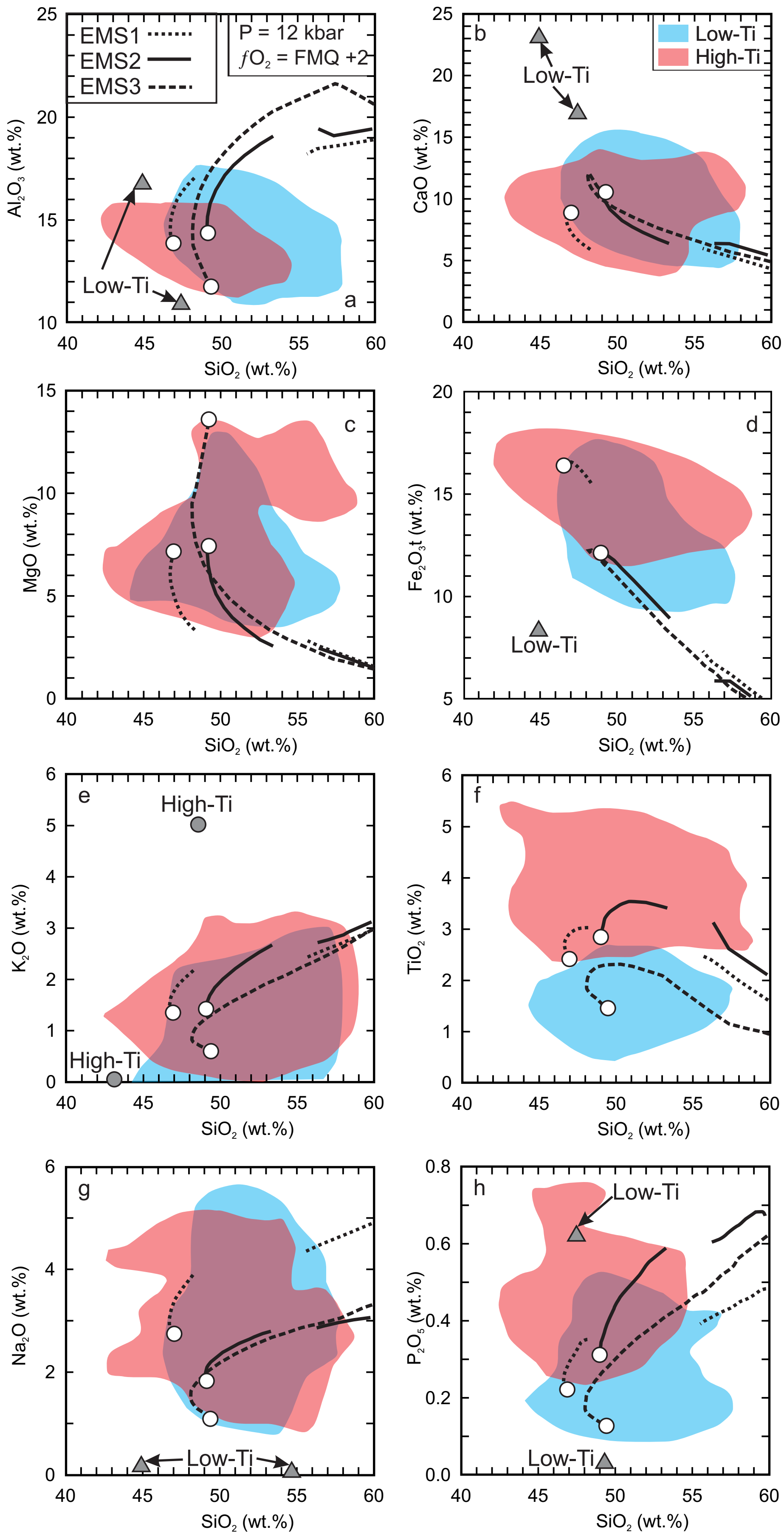
EMS1
EMS2
EMS3
P = 12 kbar
fO_2 = FMQ +2
Low-Ti
High-Ti
Al_2O_3 (wt.%)
CaO (wt.%)
MgO (wt.%)
Fe_2O_3t (wt.%)
K_2O (wt.%)
TiO_2 (wt.%)
Na_2O (wt.%)
P_2O_5 (wt.%)
SiO_2 (wt.%)
a
b
c
d
e
f
g
h

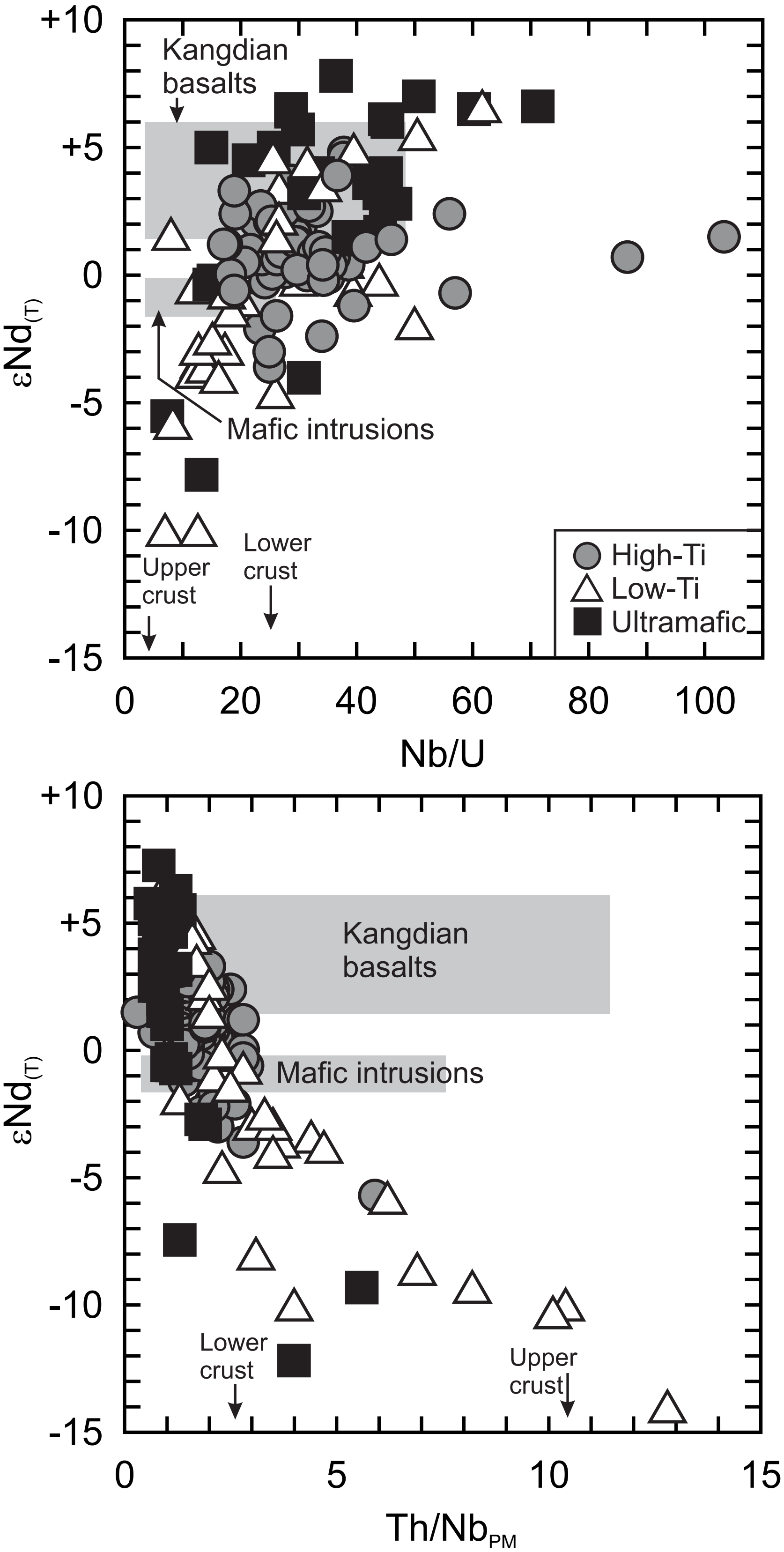
+10
+5
0
-5
-10
-15
εNd(T)
Kangdian
basalts
Mafic intrusions
Upper
crust
Lower
crust
High-Ti
Low-Ti
Ultramafic
0
20
40
60
80
100
Nb/U
+10
+5
0
-5
-10
-15
εNd(T)
Kangdian
basalts
Mafic intrusions
Lower
crust
Upper
crust
0
5
10
15
Th/NbPM

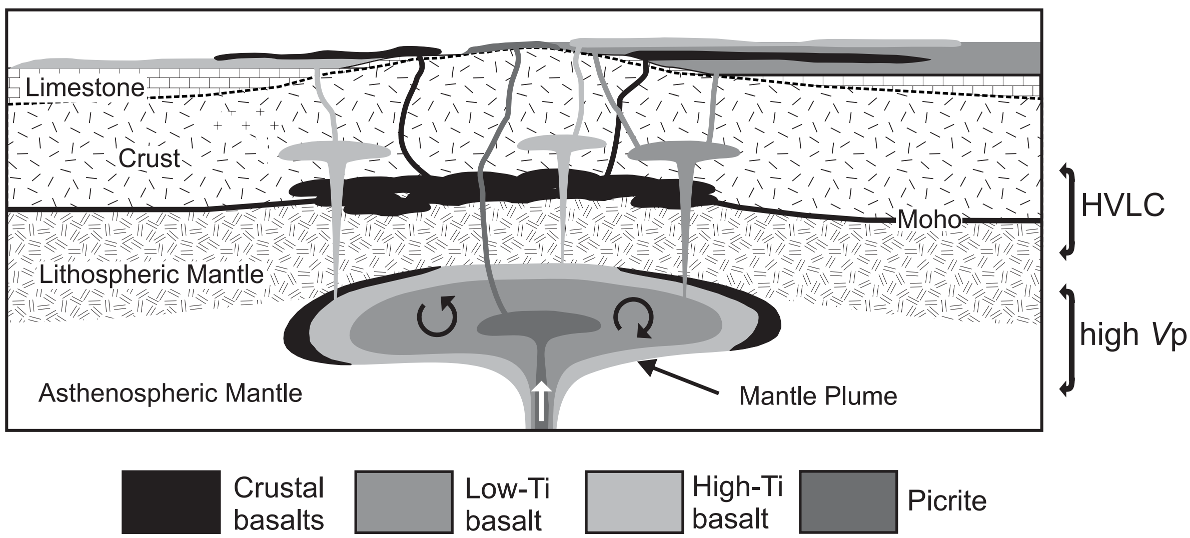

Limestone
Crust
Moho
Lithospheric Mantle
Asthenospheric Mantle
Mantle Plume
HVLC
high Vp
Crustal basalts
Low-Ti basalt
High-Ti basalt
Picrite

Table 1. *SHRIMP U-Pb ages of inherited zircons from the Panzhihua and Yingpanliangzi granitic plutons*

Sample	U (ppm)	Th (ppm)	Th/U	$^{207}Pb/^{206}Pb$	± 1σ	$^{207}Pb/^{235}U$	± 1σ	$^{206}Pb/^{238}U$	± 1σ	error corr.	$^{206}Pb/^{238}U$ (Ma ± 1σ)	$^{207}Pb/^{206}Pb$ (Ma ± 1σ)
Panzhihua												
GS03-010-2	489	266	0.56	0.0675	0.0011	1.3280	0.0252	0.1426	0.0012	0.447	860 ± 7	854 ± 34
GS03-010-3	262	267	1.05	0.0657	0.0018	1.4060	0.0408	0.1553	0.0017	0.383	930 ± 10	797 ± 57
GS03-010-4	515	26	0.05	0.0666	0.0015	1.5690	0.0392	0.1710	0.0021	0.476	1018 ± 11	824 ± 46
GS03-010-6	435	175	0.42	0.0672	0.0013	1.3110	0.0288	0.1416	0.0014	0.440	854 ± 8	843 ± 41
Yingpanliangzi												
GS03-065-1	176	114	0.67	0.0631	0.0016	0.7800	0.0211	0.0897	0.0011	0.432	554 ± 6	711 ± 53
GS03-065-4	233	271	1.20	0.0620	0.0011	0.9380	0.0197	0.1098	0.0012	0.551	671 ± 7	674 ± 37
GS03-065-5	300	253	0.87	0.0658	0.0005	1.1790	0.0153	0.1298	0.0014	0.837	787 ± 8	801 ± 15
GS03-065-6	236	133	0.58	0.0645	0.0012	0.9040	0.0190	0.1018	0.0011	0.541	625 ± 7	757 ± 37
GS03-065-7	391	226	0.60	0.0637	0.0009	0.7790	0.0140	0.0888	0.0010	0.621	548 ± 6	731 ± 30
GS03-065-8	903	949	1.09	0.0613	0.0009	0.6600	0.0119	0.0782	0.0008	0.575	485 ± 5	649 ± 32
GS03-065-9	36	23	0.66	0.0703	0.0022	1.1960	0.0419	0.1234	0.0021	0.477	750 ± 12	937 ± 63
GS03-065-10	62	46	0.77	0.0678	0.0017	1.2030	0.0349	0.1286	0.0018	0.491	780 ± 10	863 ± 53
GS03-065-11	195	140	0.74	0.0647	0.0008	1.0560	0.0180	0.1184	0.0014	0.665	721 ± 8	765 ± 28
GS03-065-13	291	297	1.05	0.0625	0.0016	0.8080	0.0226	0.0938	0.0010	0.408	578 ± 6	690 ± 54
GS03-065-17	297	252	0.88	0.0630	0.0016	0.8780	0.0246	0.1012	0.0012	0.431	621 ± 7	707 ± 54

Table 2. *Hf isotope analyses of Neoproterozoic zircons from the Phan Si Pan granite and Tu Le rhyolite*

Sample	Rock type	Age (Ma)	$^{176}Hf/^{177}Hf$	± 1σ	$^{176}Lu/^{177}Hf$	$^{176}Yb/^{177}Hf$	T_{DM1} (Ga)	T_{DM2} (Ga)	Hf_i	$\varepsilon Hf_{(T)}$
YB24-05	Granite	789 ± 15	0.282294	0.000011	0.000800	0.024535	1.35	1.70	0.282282	+0.1
YB27-01	Granite	744 ± 13	0.282225	0.000016	0.001163	0.038888	1.46	1.89	0.282209	-3.5
YB27-11	Granite	715 ± 13	0.282193	0.000007	0.001483	0.039588	1.51	1.99	0.282173	-5.4
YB27-13	Granite	708 ± 13	0.282272	0.000021	0.000848	0.022848	1.38	1.80	0.282261	-2.5
YB29-11	Granite	816 ± 16	0.282273	0.000017	0.000660	0.026871	1.37	1.72	0.282263	0.0
LTH26A-08	Granite	632 ± 14	0.282433	0.000015	0.000541	0.017499	1.14	1.47	0.282427	+1.7
LTH26A-09	Granite	825 ± 17	0.282225	0.000015	0.000645	0.020782	1.44	1.83	0.282215	-1.5
YB12-01	Rhyolite	724 ± 14	0.282315	0.000010	0.001148	0.038304	1.33	1.70	0.282299	-0.8
YB12-04	Rhyolite	818 ± 16	0.282281	0.000010	0.001327	0.043816	1.38	1.73	0.282261	0.0
YB12-06	Rhyolite	793 ± 15	0.282281	0.000009	0.001142	0.038210	1.38	1.74	0.282264	-0.5
YB12-10	Rhyolite	708 ± 14	0.282227	0.000014	0.000648	0.021917	1.43	1.89	0.282218	-4.0
YB12-18	Rhyolite	720 ± 14	0.282261	0.000008	0.000926	0.030538	1.40	1.82	0.282248	-2.6
YB19A-01	Rhyolite	769 ± 15	0.282246	0.000012	0.000779	0.026009	1.41	1.82	0.282235	-2.0
YB19A-03	Rhyolite	795 ± 16	0.282246	0.000017	0.000877	0.029793	1.42	1.80	0.282233	-1.5
YB19A-05	Rhyolite	780 ± 16	0.282329	0.000013	0.002321	0.076132	1.35	1.67	0.282295	+0.3
YB19A-06	Rhyolite	788 ± 16	0.282299	0.000009	0.000894	0.029255	1.34	1.69	0.282286	+0.2
YB19A-07	Rhyolite	763 ± 15	0.282246	0.000010	0.001061	0.033368	1.42	1.83	0.282231	-2.3

The full dataset of the zircon ages are reported in Usuki *et al*. (2014).

Table 3. *Kangdian basalt starting compositions and modeling conditions*

Sample	04KD16-3[*]	04KD16-3 (model EMS1)	99KD22-8[+]	99KD22-82 (model EMS2)	04KD4-24[*]	04KD4-24 (model EMS3)
SiO_2 (wt%)	46.05	45.60	48.35	47.95	48.50	48.18
TiO_2	2.44	2.42	2.78	2.76	1.47	1.46
Al_2O_3	13.76	13.63	14.17	14.05	11.61	11.53
Fe_2O_3t	17.79	17.62	13.08	12.97	12.66	12.58
MnO	0.30	0.30	0.17	0.17	0.18	0.18
MgO	6.98	6.91	7.24	7.18	13.48	13.39
CaO	8.34	8.26	10.47	10.38	9.87	9.81
Na_2O	2.74	2.71	1.85	1.83	1.13	1.12
K_2O	1.36	1.35	1.40	1.39	0.62	0.62
P_2O_5	0.22	0.22	0.31	0.31	0.13	0.13
H_2O		1 wt%		1 wt%		1 wt%
fO_2		FMQ +2		FMQ +2		FMQ +2
Pressure (GPa)		1.2		1.2		1.2

Major element data for models normalized to 100% including water. [*]Data from Lin *et al*. (2007) and [+] data from Li *et al*. (2002).